2018

A High Sensitivity Temperature Sensor Based on Balloon-Shaped Bent SMF Structure with its Original Polymer Coating

Ke Tian
Harbin Engineering University, China

Gerald Farrell
Technological University Dublin, gerald.farrell@tudublin.ie

Elfed Lewis
University of Limerick, Ireland

See next page for additional authors

Recommended Citation

Tian, K., Farrell, G. & Lewis, E. (2018). A high sensitivity temperature sensor basedon balloon-shaped bent SMF structure with its original polymer coating. *Measurement Science and Technology, vol. 29, no. 8. doi:10.1088/1361-6501/aac992*

PAPER

A high sensitivity temperature sensor based on balloon-shaped bent SMF structure with its original polymer coating

To cite this article: Ke Tian *et al* 2018 *Meas. Sci. Technol.* **29** 085104

IOP Publishing Measurement Science and Technology
Meas. Sci. Technol. **29** (2018) 085104 (7pp) https://doi.org/10.1088/1361-6501/aac992

A high sensitivity temperature sensor based on balloon-shaped bent SMF structure with its original polymer coating

Ke Tian[1], Gerald Farrell[2], Elfed Lewis[3], Xianfan Wang[1], Haidong Liang[1,4] and Pengfei Wang[1,5]

[1] Key Laboratory of In-fiber Integrated Optics of Ministry of Education, College of Science, Harbin Engineering University, Harbin 150001, People's Republic of China
[2] Photonics Research Centre, Dublin Institute of Technology, Kevin Street, Dublin 8, Ireland
[3] Department of Electronic and Computer Engineering, Optical Fibre Sensors Research Centre, University of Limerick, Limerick, Ireland
[4] Hands and Feet Microsurgery, the Second Hospital of Dalian Medical University, Dalian 116023, People's Republic of China
[5] Key Laboratory of Optoelectronic Devices and Systems of Ministry of Education and Guangdong Province, College of Optoelectronic Engineering, Shenzhen University, Shenzhen 518060, People's Republic of China

E-mail: pengfei.wang@dit.ie

Received 7 March 2018, revised 26 May 2018
Accepted for publication 1 June 2018
Published 28 June 2018

Abstract

A high sensitivity optical fibre temperature sensor is demonstrated based on a balloon-shaped bent single-mode (BSBS) fibre structure where the fibre retains its original protective polymer coating. The BSBS fibre structure can be simply realized by bending a coated straight single-mode fibre into the balloon shape using a section of silica capillary tube. By adjusting the bending radius of the balloon-shaped fibre section, a modal interferometer between the core mode and the coating mode can be effectively implemented at a suitable bending radius. Considering the intrinsically high thermo-optical coefficient and thermal expansion coefficient of the polymer coating, the BSBS fibre structure offers excellent temperature sensing performance. Experimental results show that the temperature sensitivity is as high as -2465 pm °C^{-1} with a resolution of 0.008 °C over the temperature range of 20.7 °C–31.7 °C. Based on its simple fabrication process, very low cost, and experimentally determined high sensitivity coupled with good repeatability, the temperature sensor described in this article could be a competitive candidate in many temperature sensing applications.

Keywords: modal interferometer, fibre bend, polymer coating, temperature measurement

(Some figures may appear in colour only in the online journal)

1. Introduction

Accurate temperature measurement has played an important role in a range of industrial applications for many years. Optical fibre-based temperature sensors have attracted significant research attention due to their inherent advantages of compactness, real-time response and natural immunity to external electromagnetic interference. To date, a series of temperature sensors have been developed based on fibre grating structures including fibre Bragg gratings (FBGs) [1] and long-period gratings (LPGs) [2], as well as some special fibre structures e.g. those based on multicore fibre [3], hollow core fibre [4] and photonic crystal fibre (PCF) [5]. Fibre grating-based temperature sensors are compact and are relatively easily fabricated using mature manufacturing techniques. However, basic grating-based fibre temperature sensors only offer relatively low measurement sensitivity and limited accuracy of about ±0.1 °C. Temperature sensors based on special fibres

possess better measurement characteristics and performance, but at the expense (of the fibre) and the need for complicated fabrication processes which have hindered their application in practical production and applications.

In recent years, fibre interferometer-based temperature sensors have become increasingly popular because of a number of significant advantages over other conventional configurations, such as compact structure, high sensitivity and high stability in hostile environments. A variety of fibre interferometers have been successfully developed into temperature sensors, for instance, Sagnac interferometers [6, 7], Mach–Zehnder interferometers (MZIs) [8, 9], Fabry–Perot interferometers (FPIs) [10, 11] and Michelson interferometers [12, 13]. These interferometer-based temperature sensors can offer acceptable sensitivity, but their disadvantages include fragility, complex pre-processing that often requires the use of expensive infrastructure such as femtosecond lasers or highly accurate tapering facilities, all of which limit their development in real sensor systems. Therefore, the effective fabrication of a fibre interferometer in a simple repeatable manner is a significant goal in many research projects. Single-mode fibre (SMF) bend formed modal interferometers provide a potential solution to this problem because they are inherently simple structures and are easy to fabricate. However, in previous cases, the SMF bend induced interference dip has often exhibited a relatively poor extinction ratio of about 5 dB [14–16] and as a result the temperature sensing performance is also unsatisfactory resulting in a sensitivity of only -26.5 pm $°C^{-1}$ [15]. Polymer coatings are sometimes used to improve the temperature sensing performance of optical fibre sensors [17, 18]. In the investigation described in this article, it was determined that the original manufacturers' protective polymer coating for an SMF is a good choice and more importantly, by using the original coated polymer instead of other post-coating polymer materials, the fabrication process of the sensor is greatly simplified. In addition, this approach also offers a very uniform coating thickness which cannot easily be achieved by other post-coating methods.

In this article, a high sensitivity fibre optic temperature sensor based on a balloon-shaped bent single-mode (BSBS) fibre structure with its original polymer coating is described. The schematic configuration of the sensor structure is shown in figure 1. The BSBS fibre structure is composed of a length of unstripped SMF, and a capillary tube is used to bend the length of SMF into a balloon shape. With a suitable bending radius, a modal interferometer can be effectively established based on the propagating core mode and the excited coating modes. Compared with the uncoated BSBS fibre structure, the structure of the sensor of this investigation achieves better temperature sensing performance which can be attributed to the high thermo-optical coefficient (TOC) and thermal expansion coefficient (TEC) of the polymer coating. Experimental results demonstrate its high temperature sensitivity and good repeatability over the temperature range of 20.7 °C–31.7 °C. In addition to the direct advantage of high sensitivity, temperature sensor of this investigation also includes a simple fabrication process and ultra-low cost which makes it highly suitable as a competitive sensor in the field of temperature measurement.

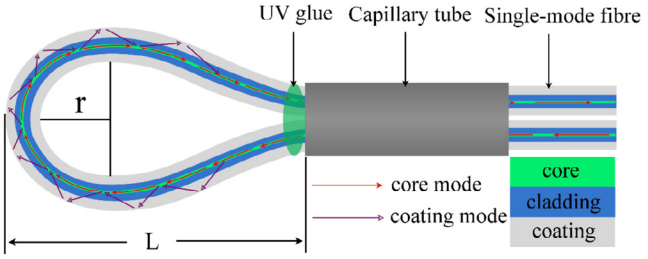

Figure 1. Schematic diagram of the proposed sensor structure.

2. Principle and analysis

For a commercial SMF-28, the coating layer is generally made of an acrylate polymer material, and it has a relatively uniform coating thickness of 62.5 ± 2.5 μm. Figure 1 illustrates the schematic diagram of the polymer coated BSBS fibre modal interferometer configuration. The bending radius and the length of the balloon-shaped section are defined as r and L, respectively. As shown in figure 1, the light initially propagates along the input straight section of the SMF as a core mode. When the light arrives at the balloon-shaped section, due to the bend in the waveguide, a portion of the light is coupled into the cladding and further coupled into the coating at which point it excites coating modes. These excited coating modes propagate within the SMF coating, when they reach the coating/air border, a portion of their mode energy is reflected back to the fibre core. As the light continues to propagate along the bent fibre section, periodic reflection between the core and the coating occurs. Hence, a modal interferometer is formed because of the different in the effective refractive indexes (RIs) and the optical paths lengths experienced by the light signals propagating in the core mode and the coating modes. In the case of a typical two-mode formed modal interferometer, the output intensity can be expressed by [19]:

$$I_{\text{out}} = I_{\text{core}} + I_{\text{coating}} + 2\sqrt{I_{\text{core}} I_{\text{coating}}}\cos(\varphi + \varphi_0) \quad (1)$$

where I_{core} and I_{coating} is the intensity of the core mode and the coating mode, respectively, and φ_0 is the initial phase. φ is the phase difference between the core mode and the coating mode which can be expressed as [20]:

$$\varphi = \frac{2\pi L_{\text{eff}}}{\lambda} \Delta n_{\text{eff}}. \quad (2)$$

Where L_{eff} is the effective bent length, $\Delta n_{\text{eff}} = n_{\text{eff}}^{\text{core}} - n_{\text{eff}}^{\text{coating}}$ is the effective refractive index (RI) difference between the core and coating mode, and λ is the free space wavelength. When the phase difference meets the condition of $\varphi = (2m + 1)\pi$, $m = 0, 1, 2\ldots$, an interference dip appears at certain wavelengths [21], defined by:

$$\lambda_m = \frac{2L_{\text{eff}} \Delta n_{\text{eff}}}{2m + 1}. \quad (3)$$

When the surrounding temperature varies, the value of Δ_{neff} and L_{eff} also change because of the well-known thermo-optic

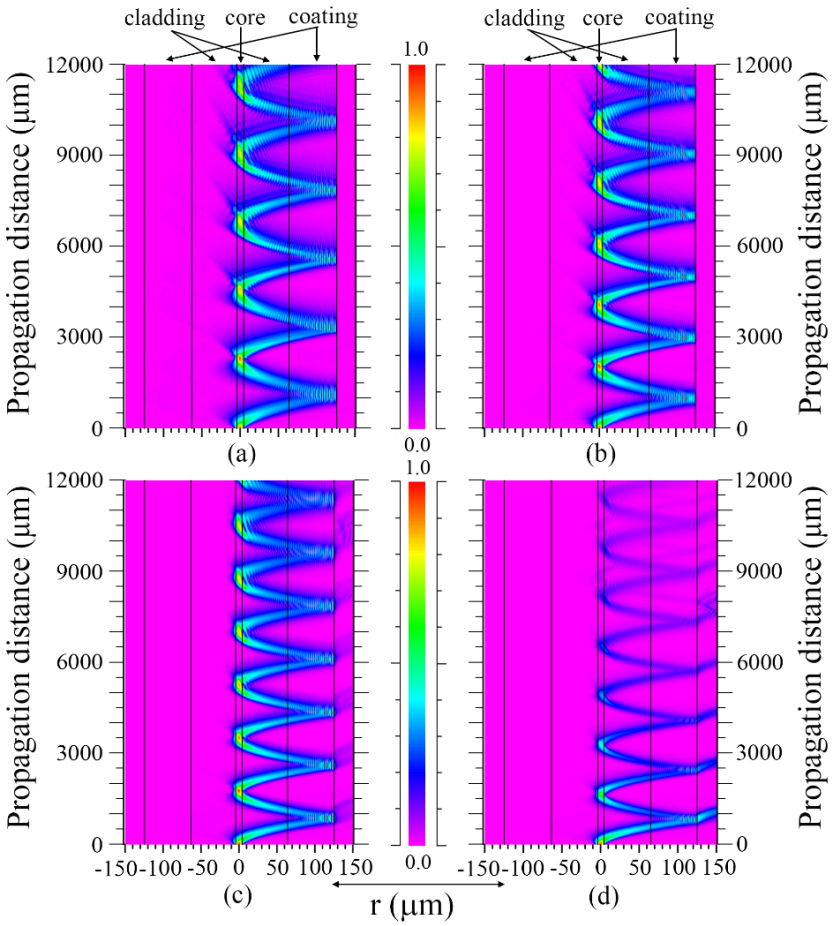

Figure 2. The optical intensity distribution of the sensor structure (at the most curved section) with different bending radii (a) $r = 5$ mm; (b) $r = 4$ mm; (c) $r = 3$ mm; (d) $r = 2.7$ mm.

and the thermal expansion effect of materials, and the resulting relative wavelength shift can be expressed as [22]:

$$\frac{\Delta\lambda}{\lambda}(\xi + \alpha)\,\Delta T \tag{4}$$

where ζ and α are the TOC and the TEC of the materials, respectively. As the polymer coating has higher TOC and TEC values than the silica fibre, the temperature sensitivity is therefore improved.

To investigate the spatial optical intensity distribution within the bent fibre (at the most curved section) and the effect of bending radius on it, numerical simulations based on the beam propagation method (BPM) have been performed. The specific simulation parameters used were: the diameter and RI for the SMF core and cladding are 8.3/125 μm and 1.4504/1.4447, respectively, and the RI of the polymer coating is assumed to be 1.51. The simulation length of SMF is 12 mm and the free space wavelength was set at 1550 nm. When the bending radii were set as 5 mm, 4 mm, 3 mm and 2.7 mm, the calculated results are presented in figures 2(a)–(d), respectively. From figure 2, it is clear that the optical intensity within the bent fibre is mainly concentrated on the outer side of the bend. Furthermore, considering the optical intensity distribution, it is also clear that light reflection exists between the fibre core and polymer coating, which in turn results in a transmission spectrum which possesses distinct dips at certain wavelengths as a result of interference. From figures 2(a)–(d), it can be seen that when the bending radius decreases, the numbers of reflections within the bent region increases which in turn contributes to increased interference and potentially increased sensitivity. However, when the bending radius is too small, the light energy leaks out of the coating, which can be clearly observed from figures 2(c) and (d). Therefore, an appropriate bending radius needs to be confirmed experimentally to achieve an effective interference pattern.

Prior to a more formal experimental investigation described in the next section and based on the above theoretical analysis and numerical simulations, the transmission spectrum (1520 nm–1600 nm) of a bent fibre structure for different bending radii was investigated experimentally. In this investigation, when the bending radius of the SMF was more than 5 mm, no interference pattern appears within the wavelength range since little or no light energy in the fibre core is coupled into the cladding and coating. The bending radius was decreased from 5 mm to 3.5 mm with a step of 0.5 mm, and the measured results are shown in figure 3. From figure 3, it can be observed that with a decreasing bending radius, the intensity loss of the transmission spectrum increases because more light is coupled into the coating. When the bending radius reaches 5 mm and 4.5 mm, interference fringes appeared, but

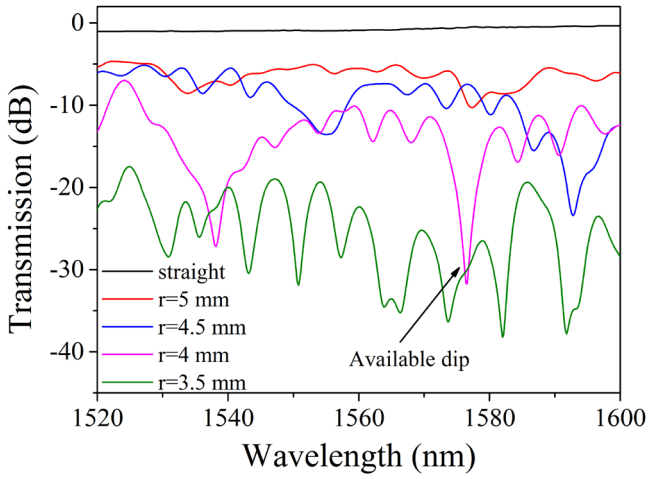

Figure 3. Transmission spectrum of the polymer coated BSBS fibre structure with different bending radii.

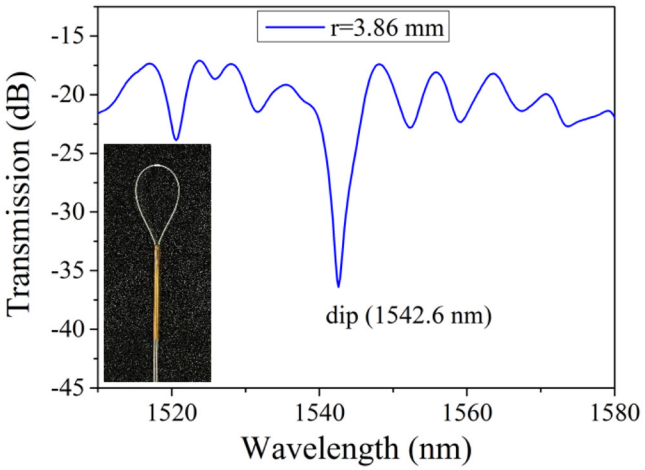

Figure 4. The transmission spectrum of the BSBS fibre structure with the bending radius of 3.86 mm, the inserted picture is the experimentally fabricated sample.

possessing a relatively low extinction ratio. With a further decrease of the bending radius to 4 mm, an interference dip appeared which has a relatively large extinction ratio (more than 15 dB). As the bending radius was further decreased to 3.5 mm, more interference dips were detected which means that the free spectral range (FSR) of the transmission spectrum decreases. Moreover, the extinction ratio of these interference dips becomes smaller. If the bending radius continues to decrease, excess light is coupled into the coating and even leaks out from the coating resulting in a large loss. Ultimately, these initial experiments determined that an appropriate bending radius to form a modal interferometer should lie around the region of 4 mm. In the next section, a more detailed experiment is described where a robust bent fiber structure is fabricated based on the use of a capillary tube and UV glue.

3. Experiments and discussion

To fabricate a robust and mechanically stable sensor structure, both ends of the SMF-28 were inserted into a silica capillary tube of length 1.5 cm and inner diameter 600 μm. By moving the silica capillary tube along the fibre, the bending radius of the balloon-shaped section was flexibly adjusted. When a preferred bending radius was reached, ultraviolet (UV) glue was used to immobilize the sensor structure. The entire fabrication process is extremely simple and can even be completed without the use of a fusion splicer. The image of the fabricated sensor sample is shown in the insert in figure 4. Two bend parameter values were measured, the bending radius r value of 3.86 mm (the bending radius was adjusted to 3.86 mm to obtain the optimum interference dip condition) and the length of the balloon-shaped section L which is 13.42 mm. The transmission spectrum of the obtained sample was also measured and is depicted in figure 3. As shown in figure 4, several interference dips were detected over the wavelength range of 1510 nm–1580 nm. Among these interference dips, a desired dip with a central wavelength located at 1542.6 nm was chosen to perform temperature measurement since it has a relatively large extinction ratio (17.2 dB).

The experimental setup for temperature measurement using the sensor of this investigation is schematically depicted in figure 5. The fabricated sample was placed in contact with the surface of a thermoelectric Peltier cooler using a 3D displacement platform. A stable triple power supply (TTI EL302RT) was used to control the input electric current of the Peltier cooler, and the real-time temperature value of its surface was monitored using a thermocouple (RS 1313). The input SMF of the sample was connected to a broadband light source (BBS, Thorlabs S5FC1005S). The light was transmitted through the sample and finally recorded using an optical spectrum analyzer (OSA, Agilent 86142B).

The transmission spectrum evolution of the sensor when subjected to a temperature range from 20.7 °C to 30.7 °C with a step of 1 °C is depicted in figure 6(a). In order to test the repeatability of this temperature sensor, a reversed measurement cycle was applied with the temperature being decreased from 30.7 °C back to 20.7 °C, and the result is depicted in figure 6(b). As shown in figure 6(a), the selected dip has a clear wavelength shift (27 nm) as the temperature was increased from 20.7 °C to 30.7 °C. When the temperature was decreased, the evolution of the dip feature was reversed compared with the temperature increase process, as presented in figure 6(b).

The resulting wavelength shift of the dip for the temperature increase and decrease processes were plotted and fitted against the temperature in figure 7. From figure 7, both characteristics exhibit a high linear regression coefficient value (R^2) of 0.9980 and 0.9991, and the temperature sensitivities at the temperature increase and decrease processes were determined as -2465 pm °C^{-1} and -2445 pm °C^{-1}, respectively. Based on the transmission spectrum feature evolution with temperature and the determined sensitivities, it is also demonstrated that the temperature sensor of this investigation offers good repeatability on account of the very small differences between the results for the temperature increasing and decreasing cases. Furthermore, given that the 20 pm resolution of OSA used in the experiment, the temperature measurement resolution of this sensor system is estimated to be 0.008 °C.

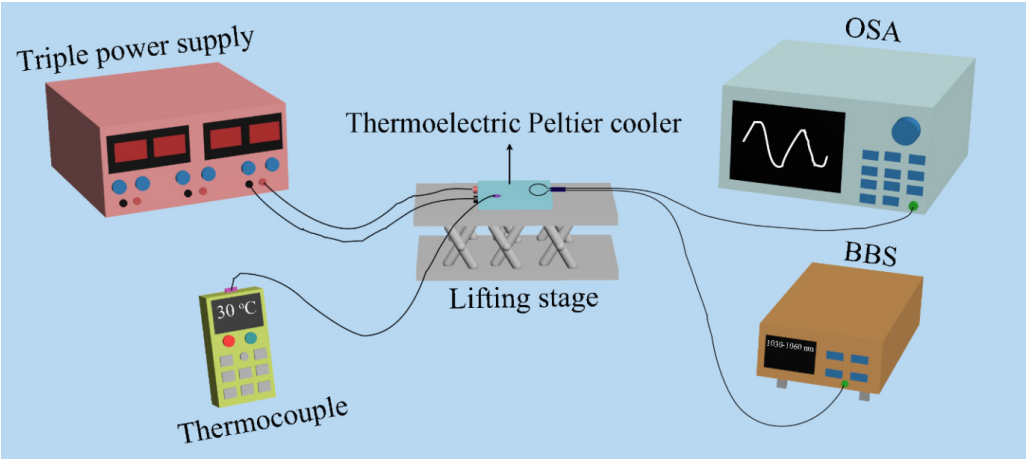

Figure 5. Schematic diagram of the experimental setup for temperature measurement.

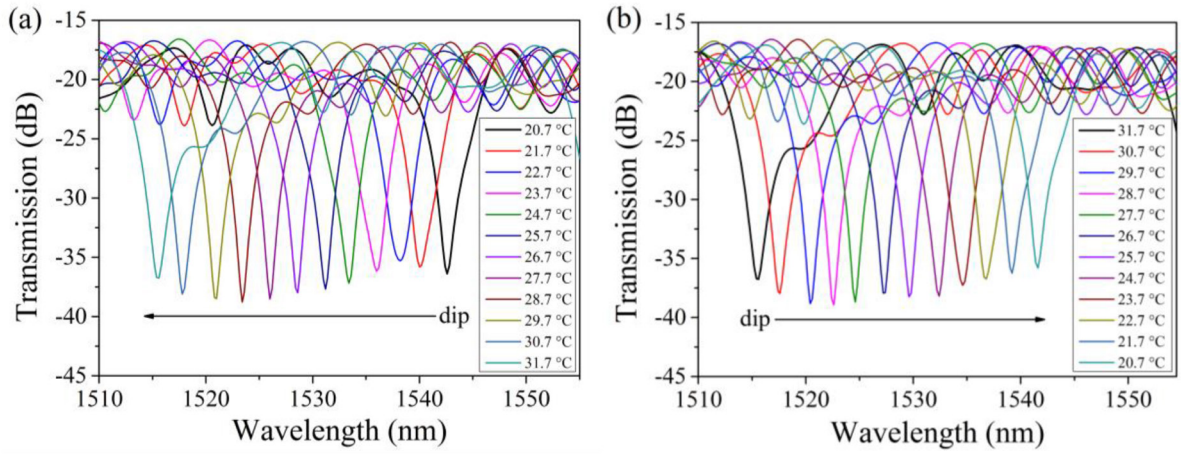

Figure 6. The transmission spectrum evolution as temperature is changed (a) temperature increases; (b) temperature decreases.

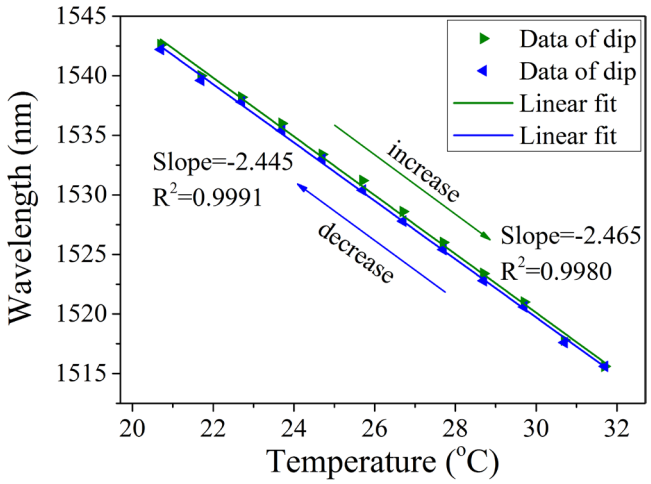

Figure 7. Linear fitting curves of dip shifts against temperature variation.

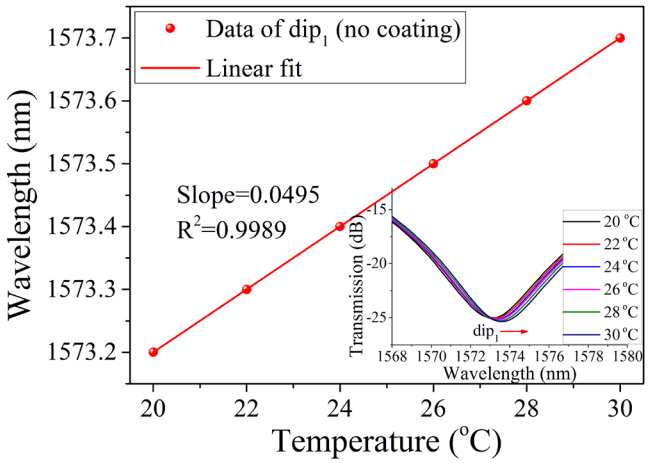

Figure 8. Linear fitting curve of dip_1 (no coating case) versus temperature variation, inset: the corresponding spectral evolution.

To confirm the improved temperature sensing performance induced by the polymer coating of optical fibres, a comparison experiment using a stripped SMF based BSBS fibre structure was performed. When the bending radius r of the BSBS fibre structure was adjusted to 4.31 mm, an available interference dip_1 with a central wavelength of 1573.2 nm was used to perform temperature sensing measurements. The corresponding dip wavelength redshifts as a function of temperature changes are shown in figure 8. From the linear fitting results, one can see that the temperature sensitivity of the bare BSBS fibre structure was determined as 49.5 pm $°C^{-1}$. Compared with the BSBS fibre structure with coating layers presented

Table 1. Comparison of the performance of different temperature sensors.

Measurement configuration	Sensitivity (pm °C^{-1})	Resolution (°C)	Ref.
FBG	12	0.8	[1]
LPG	80	0.3	[2]
Multicore fibre	28.7	Not given	[3]
Hollow core fibre	11	Not given	[4]
PCF	6600	0.015	[5]
Alcohol-filled PCF	−1170	0.085	[6]
Alcohol-filled side-hole fibre	86.8	0.23	[7]
Waist-enlarged fibre	70	Not given	[8]
Core-offset fibre with FBG	46.2	0.43	[9]
Gourd-shaped microfibre	17.15	1.17	[10]
Hybrid FPI	13	1.54	[11]
Circular optical fibre	15	Not given	[12]
Peanut-shaped fibre	96	0.26	[13]
Modal interferometer	−26.5	0.75	[15]
Side-polished fibre with polymer coating	−710	1	[17]
Tapered fibre with polymer coating	3101.8	Not given	[18]
BSBS fibre structure with polymer coating	−2465	0.008	This work

above, it is clearly to understand that the temperature sensitivity of the BSBS fibre structure was greatly improved to over 2000 pm °C^{-1} with the presence of the polymer coating layers of the BSBS fibre structure.

Table 1 shows a comparison of the sensing performance between the temperature sensor described in this investigation and other temperature sensors also cited in this article. From table 1, it is clear that the temperature sensitivity of the sensor described in this investigation is competitive when compared with other temperature sensors. Comparing temperature measurement resolutions, the value of 0.008 °C achieved in this sensor system is the best among all the temperature sensors included in table 1. In addition to the direct advantage of high sensitivity and good resolution, this proposed sensor can be fabricated using a very simple process, in return it results in lower cost compared with the other temperature sensors. It is noteworthy that the detectable temperature range in this investigation is limited by the effective working temperature of the polymer coating and the UV glue. The application areas for the sensor lie in areas which demand temperature measurement with very high resolution, to detect minute changes in temperature, for example in medical and biological diagnostics.

It should also be noted that the values of RI, TOC and TEC of the polymer coating of SMFs are likely to vary from the acrylate polymer material formulations provided by the optical fibre manufacturers. As a result, the temperature sensing performance of the BSBS fibre structures constructed using SMFs from different optical fibre manufacturers can be different. To investigate this, a comparison experiment by using a standard SMF provided by the other optical fibre manufacturer (Yofc, China) was carried out. To maintain the consistency of sensor fabrication, the bending radius was carefully adjusted to the same value of 3.86 mm. The resulting interference dip and its temperature dependent results are shown in figure 9. From figure 9, one can see that when the surrounding temperature

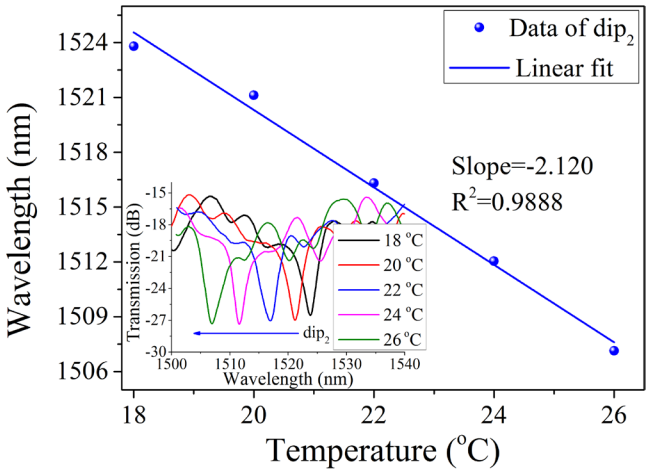

Figure 9. Linear fitting curve of dip$_2$ versus temperature variation, inset: the corresponding spectral evolution.

was increased from 18 °C to 26 °C, the interference dip$_2$ had a significant blue-shift from 1523.8 nm to 1507.14 nm, and a temperature sensitivity of −2120 pm °C^{-1} was achieved. The discrepancies of the interference dips wavelength location and the temperature sensitivities presented between figures 4 and 9 were mostly induced by the different formulations of the polymer coating materials used by the two optical fibre manufacturers. Therefore, in order to guarantee the consistency of reproductivity, it is important to use the same SMF to ensure sensing repeatability performance of the BSBS fibre structure based fibre optic sensors.

4. Conclusion

A high sensitivity optical fibre temperature sensor based on a BSBS fibre structure with its original polymer coating has been described. Through bending an unstripped SMF into a balloon shape with the help of a section of silica capillary tube,

a modal interferometer formed by the core mode and coating modes was established at a certain bending radius. Owing to the presence of the original polymer coating, the sensor of this investigation experimentally achieved a high temperature sensitivity of −2465 pm °C^{-1} coupled with a resolution of 0.008 °C over the temperature range of 20.7 °C–31.7 °C. Given its simple fabrication process, ultra-low cost and experimentally determined high sensitivity and good repeatability, this temperature sensor offers good potential as a competitive candidate for accurate temperature measurement.

Acknowledgments

This work was supported by the National Key R&D Program of China under Grant NO. 2016YFE0126500, the National Natural Science Foundation of China (NSFC) under Grant No. 61575050, the Key Program for Natural Science Foundation of Heilongjiang Province of China under Grant No. ZD2016012, the Open Fund of the State Key Laboratory on Integrated Optoelectronics under Grant No. IOSKL2016KF03, the 111 project under Grant No. B13015, the Government of Ireland International Scholarship programme, and the PhD Student Research and Innovation Fund of the Fundamental Research Funds for the Central Universities (HEUGIP201820).

ORCID iDs

Ke Tian https://orcid.org/0000-0003-0954-9350

References

[1] Liao C, Wang Y, Wang D and Yang M 2010 Fiber in-line Mach–Zehnder interferometer embedded in FBG for simultaneous refractive index and temperature measurement *IEEE Photonics Technol. Lett.* **22** 1686–8
[2] Zeng H *et al* 2016 Combining two types of gratings for simultaneous strain and temperature measurement *IEEE Photonics Technol. Lett.* **28** 477–80
[3] Antonio-Lopez J E, Eznaveh Z S, LiKamWa P, Schülzgen A and Amezcua-Correa R 2014 Multicore fiber sensor for high-temperature applications up to 1000° C *Opt. Lett.* **39** 4309–12
[4] Anand V, Mathew S, Samuel B, Radhakrishnan P and Kailasnath M 2017 Thermo-optic tuning of whispering gallery mode lasing from a dye-doped hollow polymer optical fiber *Opt. Lett.* **42** 2926–9
[5] Qian W *et al* 2011 High-sensitivity temperature sensor based on an alcohol-filled photonic crystal fiber loop mirror *Opt. Lett.* **36** 1548–50
[6] Zhao C-L *et al* 2012 Phenomenon in an alcohol not full-filled temperature sensor based on an optical fiber Sagnac interferometer *Opt. Lett.* **37** 4789–91
[7] Xin Y, Dong X, Meng Q, Qi F and Zhao C-L 2013 Alcohol-filled side-hole fiber Sagnac interferometer for temperature measurement *Sensors Actuators* A **193** 182–5
[8] Geng Y, Li X, Tan X, Deng Y and Yu Y 2011 High-sensitivity Mach–Zehnder interferometric temperature fiber sensor based on a waist-enlarged fusion bitaper *IEEE Sens. J.* **11** 2891–4
[9] Yao Q *et al* 2014 Simultaneous measurement of refractive index and temperature based on a core-offset Mach–Zehnder interferometer combined with a fiber Bragg grating *Sensors Actuators* A **209** 73–7
[10] Xian P, Feng G and Zhou S 2016 A compact and stable temperature sensor based on a gourd-shaped microfiber *IEEE Photonics Technol. Lett.* **28** 95–8
[11] Zhou A *et al* 2014 Hybrid structured fiber-optic Fabry–Perot interferometer for simultaneous measurement of strain and temperature *Opt. Lett.* **39** 5267–70
[12] Li E, Wang X and Zhang C 2006 Fiber-optic temperature sensor based on interference of selective higher-order modes *Appl. Phys. Lett.* **89** 091119
[13] Wu D, Zhu T and Liu M 2012 A high temperature sensor based on a peanut-shape structure Michelson interferometer *Opt. Commun.* **285** 5085–8
[14] Zhang X and Peng W 2015 Fiber optic refractometer based on leaky-mode interference of bent fiber *IEEE Photon. Technol. Lett.* **27** 11–4
[15] Zhao Y, Liu X, Lv R-Q and Wang Q 2017 Simultaneous measurement of RI and temperature based on the combination of Sagnac loop mirror and balloon-like interferometer *Sensors Actuators* B **243** 800–5
[16] Wang P, Rajan G, Semenova Y and Farrell G 2008 Temperature dependence of a macrobending edge filter based on a high-bend loss fiber *Opt. Lett.* **33** 2470–2
[17] Jung W-G, Kim S-W, Kim K-T, Kim E-S and Kang S-W 2001 High-sensitivity temperature sensor using a side-polished single-mode fiber covered with the polymer planar waveguide *IEEE Photonics Technol. Lett.* **13** 1209–11
[18] Hernández-Romano I, Monzón-Hernández D, Moreno-Hernández C, Moreno-Hernandez D and Villatoro J 2015 Highly sensitive temperature sensor based on a polymer-coated microfiber interferometer *IEEE Photonics Technol. Lett.* **27** 2591–4
[19] Zhang C, Zhao J, Miao C, Shen Z, Li H and Zhang M 2015 High-sensitivity all single-mode fiber curvature sensor based on bulge-taper structures modal interferometer *Opt. Commun.* **336** 197–201
[20] Tian Z *et al* 2008 Refractive index sensing with Mach–Zehnder interferometer based on concatenating two single-mode fiber tapers *IEEE Photonics Technol. Lett.* **20** 626–8
[21] Gong H, Yang X, Ni K, Zhao C-L and Dong X 2014 An optical fiber curvature sensor based on two peanut-shape structures modal interferometer *IEEE Photonics Technol. Lett.* **26** 22–4
[22] Li E 2007 Temperature compensation of multimode-interference-based fiber devices *Opt. Lett.* **32** 2064–6